Research Paper

A dual attack on the peroxide bond. The common principle of peroxidatic cysteine or selenocysteine residues

M. Dalla Tiezza[a], F.M. Bickelhaupt[b,c], L. Flohé[d,e], M. Maiorino[d], F. Ursini[d], L. Orian[a,*]

[a] *Dipartimento di Scienze Chimiche, Università degli Studi di Padova, Via Marzolo 1, 35131, Padova, Italy*
[b] *Department of Theoretical Chemistry and Amsterdam Center for Multiscale Modeling (ACMM), Vrije Universiteit Amsterdam, De Boelelaan 1083, 1081 HV, Amsterdam, the Netherlands*
[c] *Institute for Molecules and Materials (IMM), Radboud University, Heyendaalseweg 135, 6525 AJ, Nijmegen, the Netherlands*
[d] *Dipartimento di Medicina Molecolare, Università degli Studi di Padova, V.le G. Colombo 3, 35121, Padova, Italy*
[e] *Departamento de Bioquímica, Universidad de la República, Avda. General Flores 2125, 11800, Montevideo, Uruguay*

A B S T R A C T

The (seleno)cysteine residues in some protein families react with hydroperoxides with rate constants far beyond those of fully dissociated low molecular weight thiol or selenol compounds. In case of the glutathione peroxidases, we could demonstrate that high rate constants are achieved by a proton transfer from the chalcogenol to a residue of the active site [Orian et al. Free Radic. Biol. Med. 87 (2015)]. We extended this study to three more protein families (OxyR, GAPDH and Prx). According to DFT calculations, a proton transfer from the active site chalcogenol to a residue within the active site is a prerequisite for both, creating a chalcogenolate that attacks one oxygen of the hydroperoxide substrate and combining the delocalized proton with the remaining OH or OR, respectively, to create an ideal leaving group. The "parking postions" of the delocalized proton differ between the protein families. It is the ring nitrogen of tryptophan in GPx, a histidine in GAPDH and OxyR and a threonine in Prx. The basic principle, however, is common to all four families of proteins. We, thus, conclude that the principle outlined in this investigation offers a convincing explanation for how a cysteine residue can become peroxidatic.

1. Introduction

Already centuries ago, when Thénard discovered hydrogen peroxide (H_2O_2) [1], it became obvious that this compound was readily decomposed by organic material. Over the years, the observation was reported many times [2–4] and finally culminated in the discovery of catalase as a widely distributed enzyme that catalyzed the destruction of H_2O_2 [5]. Starting in the 1920s, the iron and heme content of catalase and peroxidases was established by different groups (reviewed in Refs. [6,7]), and for long, peroxidase activities were considered to strictly depend on heme as prosthetic group. Up to the mid-1970s this dogma is still reflected in monographs on oxidoreductases or reviews on catalase or peroxidases in general [8,9], although it should have been abandoned when Mills, in 1957, described glutathione peroxidase (GPx) as a non-heme protein [10]. GPx (now GPx 1) was later verified as the first mammalian selenoprotein to be discovered [11–13]. The redox-active residue in its reaction center proved to be a selenocysteine [14,15]. These findings and the later discovery of the second

mammalian selenoprotein [16], phospholipid hydroperoxide glutathione peroxidase (PHGPx, now GPx4) supported the believe that the magic catalytic power of selenium could substitute for heme in the catalytic decomposition of hydroperoxides, an assumption that had to be equally refused.

When Maiorino et al. exchanged the catalytic selenocysteine of GPx4 against cysteine, the activity of this CysGPx4 enzyme was expectedly impaired [17]. However, the bimolecular rate constant for the oxidation of the enzyme by phosphocholine hydroperoxide k_{+1} was decreased by less than 3 orders of magnitude and with $5 \times 10^4 \, M^{-1} s^{-1}$ was still orders of magnitude higher than any rate constant for the oxidation of any low molecular weight thiol by a hydroperoxide (see Table 1). Moreover, naturally occurring CysGPxs, e. g. the GPx of *D. melanogaster* [18], displayed rate constants that were almost competitive with those of mammalian selenoenzymes (for review see Ref. [19]). At the latest after the discovery, in the laboratories of Bruce Ames and Earl Stadtman, of the second non-heme peroxidase family [20,21], the peroxiredoxins, which only exceptionally work by selenium catalysis

Table 1
Selected rate constants for chalcogen oxidation near physiological pH.

| Compound	Co-reactant	k_{+1} ($M^{-1}s^{-1}$)	Ref.
GSH	H_2O_2	0.9	[23]
Cysteine	H_2O_2	2.9	[23]
Selenocysteine	H_2O_2	35.4	[24]
Protein phosphatase PTP1B	H_2O_2	9–20	[25,23]
Protein phosphatase Cdc25B	H_2O_2	160	[23]
Glyceraldehydephosphate dehydrogenase	H_2O_2	~500	[23]
Transcription factor OxyR	H_2O_2	~50 000	[26]
Peroxiredoxins	H_2O_2	~10 000–40 000 000	[23,27]
Transcription factor Ohr (Prx)	Linoleic acid hydroperoxide	30 000 000	[28]
Cys-glutathione peroxidases	H_2O_2	up to 1 600 000	[19]
Glutathione peroxidase 1 (bovine)	H_2O_2	50 000 000	[29]
Glutathione peroxidase 4 (porcine)	Phoshatidylcholine hydroperoxide	14 000 000	[19]
Glutathione peroxidase 4 U→C	Phoshatidylcholine hydroperoxide	50 000	[19]

[22], it became clear that also sulfur can efficiently catalyze the reduction of hydroperoxides.

The first step of these peroxidatic reactions is an oxidation of their active site cysteine or selenocysteine to the corresponding sulfenic or selenenic acid, respectively. The latter then react with thiol groups of diverse compounds such as glutathione, SH groups of other proteins, "resolving cysteine" residues of the peroxidase itself and/or redoxins to stepwise regenerate the ground state enzyme [30]. Analogous chemistry is now increasingly considered to explain the multiple modifications of cysteine residues of regulatory proteins. However, in most of the cases, the speed of the first step, *i.e.* that of the cysteine oxidation, is comparatively low ([31,25], see also Table 1). In many cases, their "reactive cysteines" are therefore not likely oxidized directly by H_2O_2. Instead, the oxidation equivalents are transferred to these proteins, typically via hetero-dimerization followed by thiol/disulfide exchange, by oxidized thiol peroxidases, which here act as H_2O_2 sensors [32]. Such indirect oxidative thiol modification has been demonstrated for the activation of the transcription factor Yap 1 by yeast GPx 3 in *Saccharomyces cerevisiae* [33], for the reaction of transcription factor Pap 1 and the signal transducer Sty 1 with the peroxiredoxin–type Tpx1 in *Schizosaccharomyces pombi* [34], of the activator protein STAT3 with PrxII in mammalian cells (HEK293T) [35], and the *S*-glutathionylation of protein kinase C and others by glutathione *S*-transferase P [36]. More recently, Stöcker et al. [37] found the overall content of oxidized protein thiols decreased in mammalian cells having the 2-Cys-Prxs knocked-out. This surprising finding indicates that the support of thiol peroxidases in cysteine oxidation is more common than hitherto anticipated.

The cysteine residues of 2-Cys-peroxiredoxins reacting fast with H_2O_2 were the first to be called "peroxidatic cysteine" residues (C_P), but this term has meanwhile been adopted to all cysteine or selenocysteine residues (U_P in this case) with unusually high reactivity towards hydroperoxides. They do not only exist within the two thiol peroxidase families. Other well documented examples are the bacterial transcription factors of the OxyR family discovered 1985 by Ames and coworkers in *Salmonella typhimurium* [38]. Also, the active site cysteine of GAPDH is often oxidized directly by H_2O_2 or peroxynitrite. Its activity as glycolytic enzyme is thereby blocked, whereby carbohydrate metabolism is directed towards the pentose phosphate shunt, and as glutathionylated, nitrosylated or aggregated protein GAPDH adopts a broad spectrum of functions [39].

The mechanisms leading to the extreme reactivities of the cysteines (C_P) or selenocysteines (U_P) in thiol peroxidases and other proteins have only been addressed in exceptional cases. The most commonly read explanation claims surface exposure and a low pK_a of C_P or U_P, respectively, induced by neighboring basic residues. For sure, the chalcogenols in these proteins have to be dissociated to enable an efficient S_N2 attack on the hydroperoxide bond [40]. However, as is known from low molecular weight compounds with freely accessible thiols or selenols (see Table 1 and [23,41]), they will hardly react with
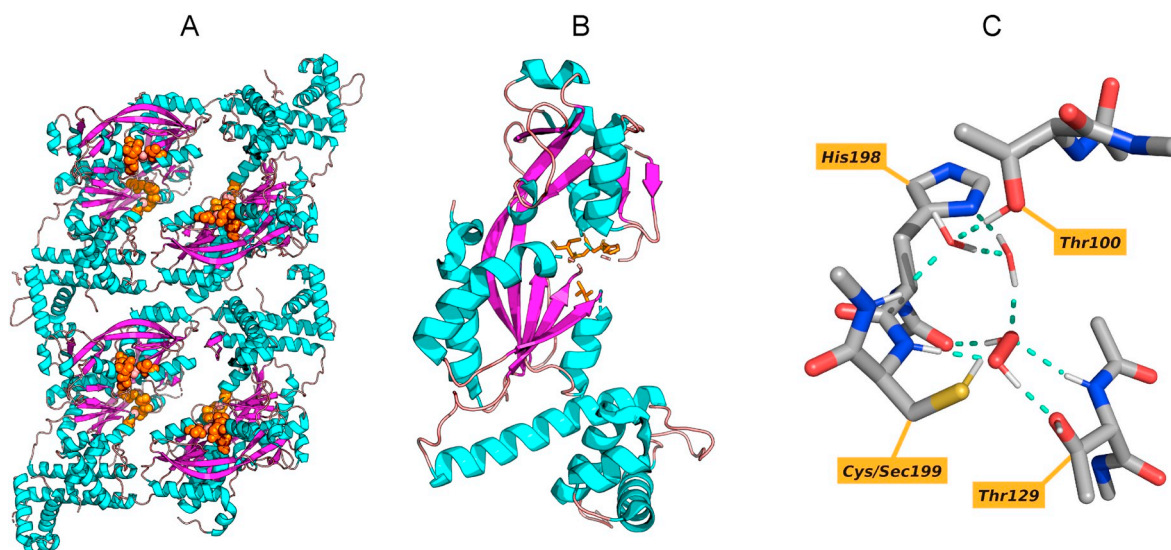
Fig. 1. A. The full-length *Pa*OxyR: the color code highlights the secondary structure and the catalytic pocket is clearly visible in orange. **B.** Zoom on the B chain; selected residues are visible in orange. **C.** The selected framework of the active site near the H_2O_2 binding site. Asp199 has been substituted by Cys/Sec199 (sulfur/selenium atom in yellow). (For interpretation of the references to color in this figure legend, the reader is referred to the Web version of this article.)

H_2O_2 at rate constants exceeding 50 $M^{-1}s^{-1}$, even if they are fully dissociated. Therefore, there is a common agreement that the peculiar architecture of the active site, which differs between protein families with a C_P (or U_P), accounts for their efficiency [25,39,40,28]. For the peroxiredoxins, a stabilization of the transition state has been postulated [25]. Peralta and coworkers [42] detected a relay of shuttling protons in GAPDH, and Ferrer Sueta et al. [40] and others highlighted the importance of an ideal leaving group.

In a previous study [43], we concluded that the unusually high efficiency of the GPx-type peroxidases is based on water-mediated proton shuttling. This leads to a zwitterionic structure, in which the O–O bond can be easily split by a concerted nucleophilic attack of the deprotonated chalcogen and an electrophilic one by a highly energized proton that is dislocated to a tryptophan nitrogen of the active site. We here try to figure out if a similar dual attack can generally account for C_P activity. To this end, we subjected the active sites of the different protein families with high C_P activity, which for convenience we call peroxidases. This way, the mechanism established for GPx family is here extended to GAPDH (1U8F), OxyR (4X6G) and an alkylhydroperoxide reductase, a peroxiredoxin (Prx; 4X0X). Although a U_P is only common in the GPx family and only exceptionally present in the Prx family, we consider Cys as well as Sec as reactive moiety of all the protein families, to gain an idea of the impact of the catalytic chalcogen on the energetics [44–46].

2. Materials and methods

Computational mechanistic studies were carried out employing state-of-the-art DFT methodologies as implemented in the Gaussian programs suite [47]. For technical limitations, we had to restrict our calculation to the intimate environment of the peroxidatic cysteine, *i.e.*, to a S (Se) distance of about 7 Å. This implies that the possible impact of the more remote residues on the reaction mechanism is ignored.

All geometry optimizations were carried out with Gaussian 16 software rev. C.01 [47] The used exchange correlation functional is the three parameters hybrid GGA B3LYP [48–51] with additional dispersion corrections implemented with the D3(BJ) approximation [52,53]. The used basis set for light atoms (H, N, C, O, S) is the Pople 6-311G (d, p) [54,55], a split-valence triple-zeta set plus p and d polarization functions for hydrogen and non-hydrogen atoms, respectively. The selenium atom, instead, has been described with Dunning's cc-pVTZ basis set [56]: a correlation-consistent and polarized-valence basis set of triple ζ quality. All the optimizations were performed in the gas phase. The stationary points, minima and transition states, have been localized

with a canonical vibrational analysis. The single normal mode associated with a negative force constant (and imaginary frequency) involved in the transition state has been verified to completely assure the nature of the barrier. Unless explicitly stated otherwise, all the geometry optimizations on the enzymes' catalytic pockets were carried out keeping a frozen backbone (N, C, O atoms are constrained). Only H, S, Se and the O atoms of the hydrogen peroxide and water molecules are free to move. In all cases, the minimum energy reaction path (MERP) has also been confirmed by a NEB (nudged elastic band) calculation carried out with ORCA 4.2.1 [57,58]. The calculations in condensed phase have been carried out with the Minnesota Solvation Model based on Density (SMD) developed by Truhlar et al. [59]. In order to mimic the proteic environment, a dielectric constant of 4.24 (diethyl ether) has been chosen in accordance with Ref [60,61]. Unless otherwise stated, only Gibbs free energies are presented in this work (additional electronic energies in gas and condensed phase are available in the supplementary information).

3. Results and discussion

In order to solve the enigma of the super-reactive cysteines in proteins, we subjected representatives of three more protein families to practically the same DFT calculations, as we had applied before for the GPx family [43]. Prerequisites for choosing the proteins were known X-ray structures and kinetics that revealed a k_{+1} for the reduction of H_2O_2 significantly higher than that of any fully dissociated low molecular mass thiol or selenol. The relevant k_{+1} values covered a wide range from comparatively low to extremely high (GAPDH: 10^2-10^4 $M^{-1}s^{-1}$; OxyR: ~10^5 M^{-1} s^{-1}; peroxiredoxins: 10^4-10^8 $M^{-1}s^{-1}$). The outcome of these calculations is described and discussed below.

3.1. PaOxyR (Pseudomonas aeruginosa oxidative stress regulator)

A common structure for the peroxide sensing in bacteria is the Oxidative Stress Regulator (OxyR), which indirectly adjusts the level of H_2O_2 in the cellular environment. It is worth to mention that sensing mechanisms in different bacteria are numerous, and the relative importance of each of them is still debated. However, two major parts of the OxyR reaction have been assessed. The reactive cysteine ("C_P") is oxidized to a sulfenic acid, but unlike in the mechanism of the selenocysteine-containing GPxs, the sulfenic acid here forms an intramolecular disulfide bridge between two highly conserved cysteines. This process leads to a structural change that results in the transcription factor activity of the (oxidized) OxyR [46]. Our attention is focused on
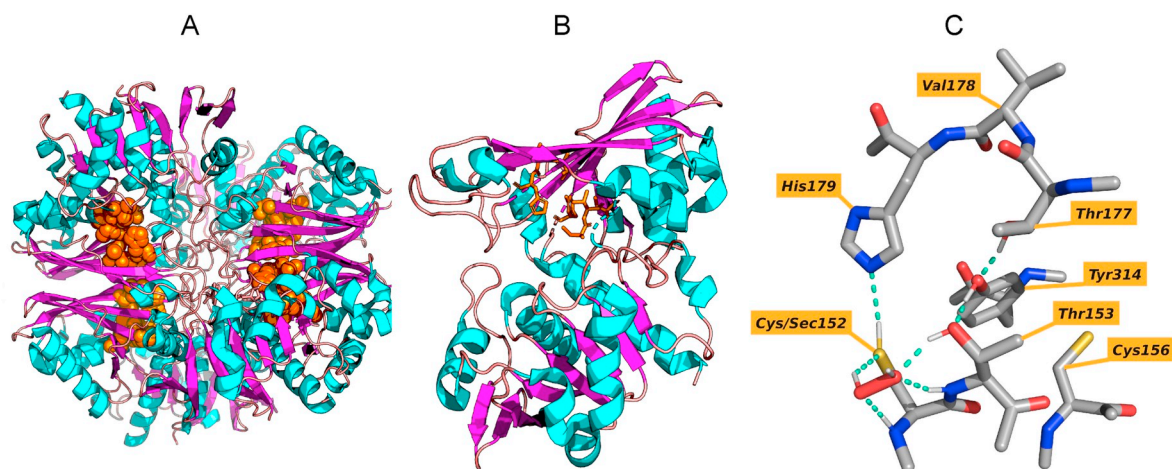
Fig. 2. A. The *Hs*GAPDH enzyme: the color code highlights the different secondary structure and the catalytic pocket are clearly visible in orange. **B.** Only the P chain is shown and the active residues are depicted with licorice style in orange. **C.** The selected framework of the active site nearby the H_2O_2 binding site. (For interpretation of the references to color in this figure legend, the reader is referred to the Web version of this article.)
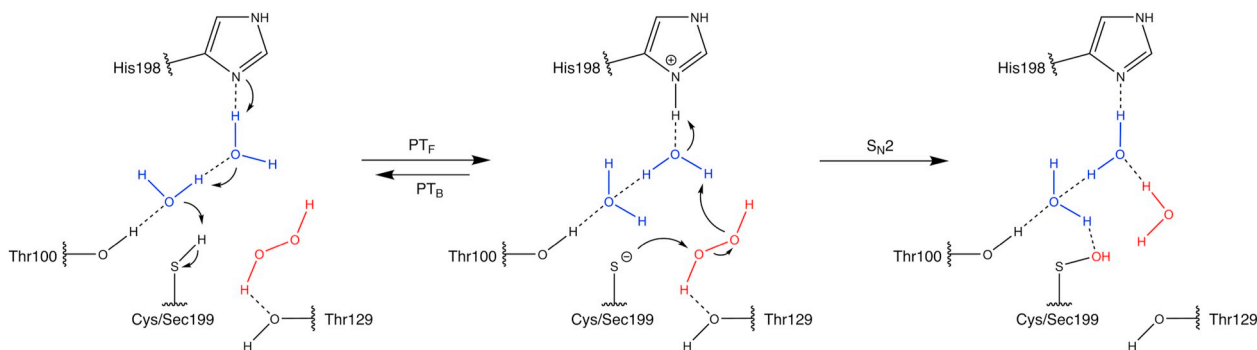
Scheme 1. Mechanism of H_2O_2 reduction in *Pa*OxyR catalytic pocket.

the first part (oxidation step), *i.e.* the H_2O_2 reduction step.

For our calculations, we selected 4 residues (Thr100, Thr129, His198 and Cys199) from the full-length *Pa*OxyR of the 4X6G crystallographic structure (Fig. 1A) [46]. In order to better understand the binding site and the orientation of the oxidizing substrate, the C_P was mutated to Asp and then the crystallized protein was exposed to H_2O_2 vapors. The entire system is tetrameric and can be further divided into two extended subunits and two contracted ones. In our initial structure, the Cys199 active site has been adapted from an Asp199 residue that was present in the *Pa*OxyR reported in Refs. [46]. In order to obtain a reliable orientation of the Cys199, the –SH moiety was kept unfrozen during our structure optimizations. The terminations of the non-contiguous amino acid chains have been saturated with the ACE/NME capping.

The chosen residues are shown in Figs. 1 B and C. Two water molecules nicely fit in the pocket in a favorable orientation to mediate a proton transfer and are also indicated. The histidine provides a good hydrogen acceptor moiety during the proton transfer while the two threonines keep the substrate and the water molecules in position. The mechanism, as it emerges from our DFT calculations, is sketched in Scheme 1. Initially, Thr129 keeps H_2O_2 close to the thiol group via H bonding, while Thr100 and His198 are connected via a two water molecule bridges. The thiol/selenol proton shuttles to the NH group of His198 with an activation energy of 31.0/25.6 kcal mol^{-1}, respectively. In case of the Cys-enzyme, the zwitterionic form is highly destabilized and the formation of the sulfenic acid occurs via a very small activation energy, *i.e.* 0.6 kcal mol^{-1}. In case of the Sec-enzyme, the zwitterionic form is even less stable and the process of proton shuttling and oxidation to selenenic acid is concerted. Notably, the S_N2 attack of the thiolate/selenolate anion to H_2O_2 is facilitated since the deprotonation has enhanced the nucleophilicity of both chalcogens. Importantly, the thermodynamic driving force for the oxidation of Sec is much larger than that computed for the oxidation of Cys, suggesting that

the presence of the heavier chalcogen in the catalytic pocket is thermodynamically as well as kinetically advantageous. To our knowledge, however, Sec variants of OxyR have so far not yet been discovered.

Based on X-ray structures and site-directed mutagenesis data, Pedre et al. [26] also postulate an essential role of Arg270. Indeed, Arg270 might offer an ultimate "parking lot" for the delocalized proton. However, we have not included this residue in the cluster essentially for two reasons: It is not close to the reactive thiol and so we can exclude a direct interaction. In addition, it interacts via N···O in *C. glutamicum* OxyR (here Arg 278) and in *P. aeruginosa* OxyR with Thr100 (Thr107 in the former structure). We therefore assume that it primarily has a structural role, but with high impact on the proton transfer mechanism. In fact, if Thr100 is free to adopt a different orientation, the two-water bridges cannot form and so the thiol proton cannot be shuttled to His to initiate the peroxidatic process (Table 2).

### 3.2. HsGAPDH (Human glyceraldehyde 3-phosphate dehydrogenase)

The glycolytic glyceraldehyde 3-phosphate dehydrogenase (*Hs*GAPDH) is a tetramer formed by four chains (O, P, Q, and R) and every subunit contains a cysteine (Cys152) that is essential for both, the aldehyde dehydrogenase activity and the fast reduction of H_2O_2. The chosen structure is the human placental *Hs*GAPDH (PDBid: 1U8F) (Fig. 2A). Like in *Pa*OxyR, the second essential amino acid is the His179, which works as hydrogen acceptor during the proton transfer step. Interestingly no water molecules are required during the reduction of the H_2O_2 substrate and this is mainly due to the presence of several hydroxyl groups, those of Thr153, Tyr314 and Thr177, which allow H-bond formation between these residues and the substrate. The selected residues for modeling the catalytic pocket are Cys152, His179, Thr153, Cys 156, Tyr314, Thr177 and Val 178 from the chain P (Figs. 2B and C). The reaction mechanism is sketched in Scheme 2.

Table 2
Forward proton transfer (PT_F), back proton transfer (PT_B) and nucleophilic substitution (S_N2) Gibbs free energies for *Pa*OxyR. ΔG_{solv} is in kcal mol^{-1}.

	Cys	Sec
	ΔG_{solv}	ΔG_{solv}
1	0.00	0.00
TS (1, 2_{CS})	30.95	25.55
2_{CS}	24.81	Direct to products
TS (2_{CS}, 3)	25.44	
3	−46.36	−54.60
$\Delta G^{\ddagger}$ (PT_F)	30.95	25.55
$\Delta G^{\ddagger}$ (PT_B)	6.14	–
$\Delta G^{\ddagger}$ (S_N2)	0.63	0.00
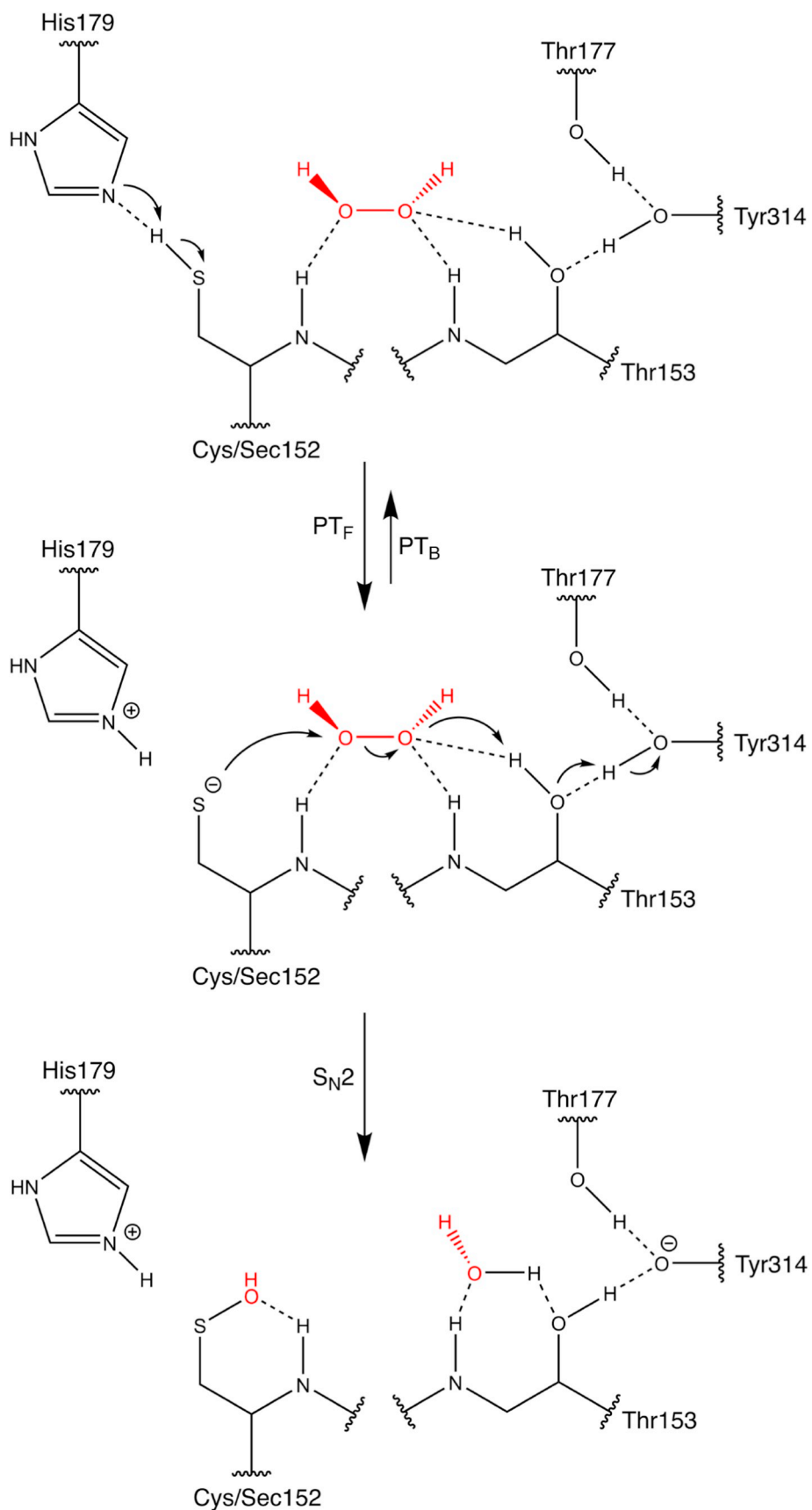
Scheme 2. Mechanism of H_2O_2 reduction in *Hs*GAPDH catalytic pocket.

The peroxide oxygens of the H$_2$O$_2$ molecule is squeezed via hydrogen bonds of the NH groups and an OH group of Thr153 and Cys/Sec152. His179 and Cys/Sec152 are in a suitable position to favor the proton shuttling. Once the thiolate/selenolate is formed, the S$_N$2 attack on the peroxide occurs, which is readily split with formation of a sulfenic (selenenic) acid. Protonation of the remaining OH by Thr153 facilitates the cleavage of water from the substrate. The latter step does not appear particularly likely, but here is facilitated by the extended hydrogen bond network, between Thr153, Thr177, Tyr314 and possibly more remote residues, which allow re-protonation of Thr153. The mechanism here calculated is practically identical to that proposed by Peralta et al., which was essentially based on molecular dynamics and bioinformatic tools [39,42].

The reaction energies are summarized in Table 3, and also in this case it emerges that the peroxide reduction is easier in presence of selenium rather than sulfur. Particularly, the barrier of the first step (proton transfer) is almost 6 kcal mol^{-1} smaller compared to that computed for the Cys-*Hs*GAPDH. The activation energy for the nucleophilic substitution is comparable between the two enzymes. Overall, however, the process is thermodynamically as well as kinetically more favored for the Sec-*Hs*GAPDH (see Table 3).

3.3. MtAhpE (Mycobacterium tuberculosis alkyl hydroperoxide reductase E)

Last, we considered an example of a peroxiredoxin subgroup, the *Mt*AhpE, in which very fast catalytic reduction of H$_2$O$_2$ and other hydroperoxides occurs [62]. The selected crystallographic structure (PDBid: 4X0X) contains four chains made by two identical subgroups: A, B and C, D (Fig. 3). The highly conserved amino acids are Cys45, Thr42, Glu48, Arg116, and Pro135. The essentiality of the residues homologous to Cys45 and Arg116 has been documented for many peroxiredoxins. Chain B has been chosen because the Arg116 orientation better resemble the conformation of the same conserved AA in other Prxs [63]. The Thr residue, which in natural peroxidoxins is sometimes exchange by serine, could be exchanged by serine in a peroxiredoxin of *Leishmania infantum* (here Thr 49), but not by any residue that lacked an OH function [64], In order to reduce the number of atoms involved and increase the chances for weak stabilizing interactions, Pro135 and Glu48 have been excluded because of the distance from the Cys45 and the residues Pro 38 and Leu 39 have been retained in the cluster because of their proximity to the reactive center. In this specific case, the used capping technique is hybrid: for terminations close to the center of the active region canonical ACE/NME residues have been used; for terminations pointing outward, a methyl substituent has been used to save computational time. The position of Arg116 is very close to Cys/Sec45: this is particularly useful because, once the chalcogenolate forms (after the proton transfer step), the positively charged Arg116 stabilizes the accumulation of electron density on the sulfur/selenium atom.

The *Mt*AhpE mechanism, sketched in Scheme 3, occurs in two steps. In the first one, a proton transfer between the donor Cys/Sec45 and the acceptor Thr42 takes place. The protonated threonine is not a commonly stable intermediate but, in this case, a stable charge separated structure is possible thanks to a synergic stabilization between the newly formed chalcogenolate and the positively charged $-OH_2^+$ moiety. A further stabilizing factor derives directly from a hydrogen bond established between the hydrogen of the charged oxygen of the threonine and the carbonyl moiety in the peptide bond of the same amino acid. H$_2$O$_2$ is bound between Thr42 and Arg116 via efficient hydrogen bonding [65,66]. The thiol/selenol is facing Thr42 in favorable position for the proton shuttling. In this first step, the barrier and the released energy values are advantageous for the Sec-enzyme by 6 kcal mol^{-1} (Table 4). The barrier for the backward proton transfer is comparable between the Cys and the Sec enzyme. Unexpectedly, the S$_N$2 step is almost barrierless (0.1 kcal mol^{-1}) for the Cys enzyme and requires a really small activation energy for the Sec variant (2.5 kcal mol^{-1}). However, the released energy is almost 10 kcal mol^{-1} larger in the latter case.

The driving force pushing towards the oxidation of the chalcogenolate is to be ascribed to two key factors: the first one involves the reaction kinetics where the competitive back proton transfer is less favored than the nucleophilic substitution with the formation of the sulfenic/selenenic acid. Then, from a thermodynamic perspective, a strong stabilization in both the cases is possible only if the reaction proceeds to the oxidation of the chalcogenolate and the formation of one water molecule. The average exergonicity of the whole process is about 70 kcal mol^{-1}.

The mechanism, as outlined above, differs from that described by Hall et al. [67]. This investigation of human Prx 5, which also considered X-ray structures of many Prxs with H$_2$O$_2$ mimics, postulate an S$_N$2 reaction between the thiolate of C$_P$ and H$_2$O$_2$ as the key peroxidatic step, which complies with our results. It further stresses the stabilization of the C$_P$ thiolate by the essential Arg, which also is in line with our results. However, it leaves open the problem, how the thiolate of C$_P$ is generated. The neighborhood of Arg is discussed, but it is not easily understood, how the guanidinium function of an Arg with a pK$_a$ around 12 should serve as a proton acceptor. Nor is it comprehensive that the very same Arg enhances the nucleophilicity of the C$_P$ sulfur and the electrophilicity of the oxygen of H$_2$O$_2$ to be attacked. Also, Zeida et al., although they applied a similar approach to the same enzyme [68] ended up with a different mechanism, which is similar to the mechanistic proposal of Hall et al. [67]. Here the essential role of Thr42 was largely ignored. At best a hydrogen bond of the threonine OH to the reacting sulfur is considered, which must be rated as unlikely, since O–H···S bonds are not readily formed. The reason for the different outcome of the calculations results from different starting conditions. In fact, the essential Arg shows relatively high RMSD value [69], which indicates the possibility of different orientations of this residue. When we started with the same Arg orientation., we could in fact reproduce

Table 3
Forward proton transfer (**PT$_F$**), back proton transfer (**PT$_B$**) and nucleophilic substitution (**S$_N$2**) Gibbs free energies for *Hs*GAPDH. ΔG_{solv} is in kcal mol^{-1}.

	Cys	Sec
	ΔG_{solv}	ΔG_{solv}
1	0.00	0.00
TS (1, 2$_{CS}$)	15.99	10.42
2$_{CS}$	−4.45	−5.08
TS (2$_{CS}$, 3)	8.99	3.79
3	−47.69	−51.22
$\Delta G^{\ddagger}$ (PT$_F$)	15.99	10.42
$\Delta G^{\ddagger}$ (PT$_B$)	20.44	15.49
$\Delta G^{\ddagger}$ (S$_N$2)	13.44	8.86

Table 4
Forward proton transfer (**PT$_F$**), back proton transfer (**PT$_B$**) and nucleophilic substitution (**S$_N$2**) Gibbs free energies for *Mt*AhpE. ΔG_{solv} is in kcal mol^{-1}.

	Cys	Sec
	ΔG_{solv}	ΔG_{solv}
1	0.00	0.00
TS (1, 2)	24.28	18.27
2	14.72	9.18
TS (2, 3)	14.82	11.66
3	−64.18	−72.32
$\Delta G^{\ddagger}$ (PT$_F$)	24.28	18.27
$\Delta G^{\ddagger}$ (PT$_B$)	9.56	9.09
$\Delta G^{\ddagger}$ (S$_N$2)	0.10	2.48
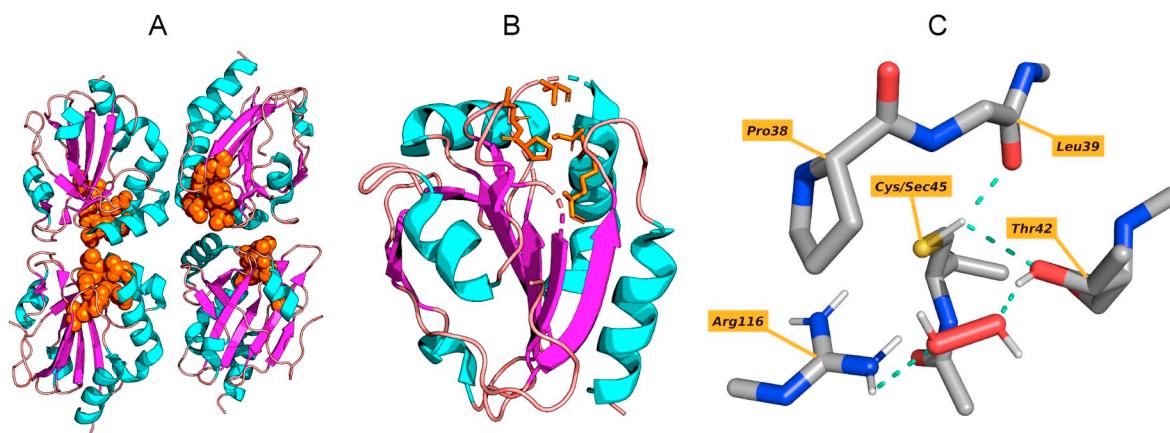
Fig. 3. A. The *Mt*AhpE enzyme: the color code highlights the different secondary structure. The AAs involved in the active area are shown in orange. **B.** The catalytic pocket of a monomer (chain B, in orange). **C.** The five conserved AAs of the selected catalytic pocket. (For interpretation of the references to color in this figure legend, the reader is referred to the Web version of this article.)
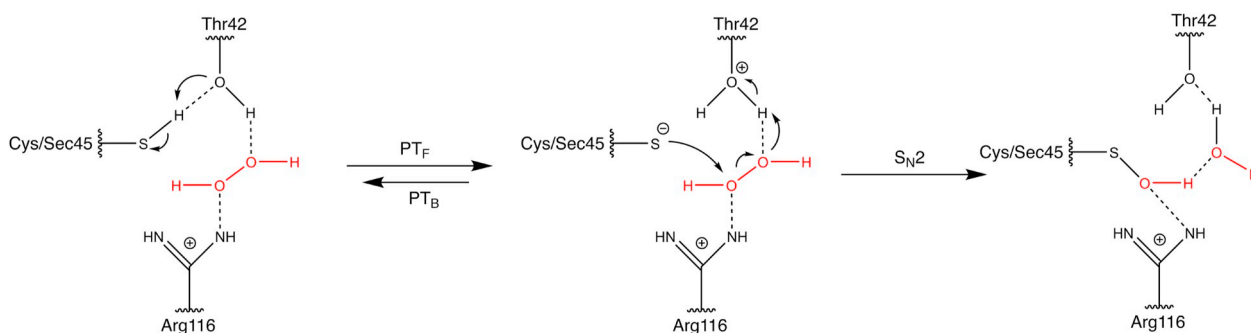
Scheme 3. Mechanism of H_2O_2 reduction in *Mt*AhpE catalytic pocket.

the results of Zeida et al. When taking the alternate Arg orientation, the role of Thr42 as proton acceptor, as shown in Scheme 3, was clearly disclosed.

4. Conclusions

For sure, the peroxidatic cysteine (C_P) or selenocysteine (U_P) has to be deprotonated to allow an efficient S_N2 reaction with the peroxide bond yielding a sulfenic or selenenic acid, and for sure, such electrophilic attack does not suffice to explain the rate constants of C_Ps or U_Ps. A second attack is required to cleave the peroxide bond efficiently.

As shown previously for the GPx family, the second attack is an electrophilic one on the second oxygen atom of the peroxide bond. Not only in the GPx family, but also in the three protein families investigated herein, the electrophilic attack is achieved by a shuttling proton, which combines with the OH or to yield water or an alcohol, respectively, as ideal leaving group.

The labile proton stems from residues of the active site and usually reaches the peroxide bond by long-range proton shuttling via water molecules (GPx), residues of the active pocket (GAPDH, Prx) or both (OxyR).

Our DFT calculations reveal that the chalcogenol proton is transferred to residues of the active site, where they form more or less stable bonds (ring nitrogen of Trp 136 in human cytosolic GPx4, His nitrogen in OxyR and GAPDH, oxygen of Thr in Prx). The proton transfer may involve more remote residues that are not considered in our calculations. In any case, it creates a zwitterionic nature of the active site.

The complex between the zwitterionic form of the proteins and the hydroperoxide reacts without any or with a very low activation energy. The activation energy appears to be lowest, if the delocalized proton is bound in an unstable, *i. e.* highly energized way (bound to Trp or Thr).

If the chalcogen is selenium instead of sulfur as in many GPxs and

sometimes in Prxs, the overall hydroperoxide reduction is thermodynamically and kinetically favored.

It remains to be demonstrated whether the emerging reaction scheme holds true for other protein families equipped with super-reactive chalcogenols. Interestingly, proton shuttling has also been implicated in the catalytic mechanism of horse radish peroxidase [70,71], suggesting that this principle may generally be helpful in splitting a peroxide bond, i.e. also in heme peroxidases.

Declaration of competing interest

None declared.

Appendix A. Supplementary data

Supplementary data to this article can be found online at https://doi.org/10.1016/j.redox.2020.101540.

References

[1] L.J. Thénard, Oservations sur des combinaisons nouvelles entrel'oxygeneet divers acides, Ann. Chem. Phys. 8 (1818) 306–312.

[2] C.F. Schönbein, Ueber die katalytische Wirksamkeit organischer Materien und deren Verbreitung in der Pflanzen- und Thierwelt, J. Prakt. Chem. 89 (1863) 323–344, https://doi.org/10.1002/prac.18630890143.

[3] G. Linossier, Contribution a l'etude des fermentsoxidants. Sur la peroxidasedu pups, C. R. Seances Soc. Biol. Fil. 50 (1898) 373–375.

[4] L. Planche, Note sur la sophistication de la Résine de jalap et sur les moyens de la reconaitre, Bull. Pharm. (Istanb.) (1810) 578–580.

[5] O. Loew, A new enzyme of general occurrence in organismis, Science 11 (1900) 701–702, https://doi.org/10.1126/science.11.279.701.

[6] C. Glorieux, P.B. Calderon, Catalase, a remarkable enzyme: targeting the oldest antioxidant enzyme to find a new cancer treatment approach, Biol. Chem. 398 (2017) 1095–1108, https://doi.org/10.1515/hsz-2017-0131.

[7] K.G. Stern, Structure and action-mechanism of hematin-containing enzymes, Yale J. Biol. Med. 10 (1937) 161–178.

[8] A. Brill, M. Florkin, E.H. Stotz, Peroxidases and catalase, Compr. Biochem. Elsevier, Amsterdam, 1966, pp. 447–479.

[9] B. Chance, G.R. Schonbaum, Catalase, The Enzymes, Academic Press, New York, 1976, pp. 362–408.

[10] G.C. Mills, Hemoglobin catabolism. I. Glutathione peroxidase, an erythrocyte enzyme which protects hemoglobin from oxidative breakdown, J. Biol. Chem. 229 (1957) 189–197.

[11] L. Flohé, The labour pains of biochemical selenology: the history of selenoprotein biosynthesis, Biochim. BBA - Gen. Subj. 1790 (2009) 1389–1403, https://doi.org/10.1016/j.bbagen.2009.03.031.

[12] L. Flohe, W.A. Günzler, H.H. Schock, Glutathione peroxidase: a selenoenzyme, FEBS Lett. 32 (1973) 132–134, https://doi.org/10.1016/0014-5793(73)80755-0.

[13] J.T. Rotruck, A.L. Pope, H.E. Ganther, A.B. Swanson, D.G. Hafeman, W.G. Hoekstra, Selenium: biochemical role as a component of glutathione peroxidase, Science 179 (1973) 588–590, https://doi.org/10.1126/science.179.4073.588.

[14] J.W. Forstrom, J.J. Zakowski, A.L. Tappel, Identification of the catalytic site of rat liver glutathione peroxidase as selenocysteine, Biochemistry 17 (1978) 2639–2644, https://doi.org/10.1021/bi00606a028.

[15] A. Wendel, B. Kerner, K. Graupe, The selenium moiety of glutathione peroxidase, in: H. Sies, A. Wendel (Eds.), Funct. Glutathione Liver Kidney, Springer Berlin Heidelberg, Berlin, Heidelberg, 1978, pp. 107–113, , https://doi.org/10.1007/978-3-642-67132-6_13.

[16] F. Ursini, M. Maiorino, C. Gregolin, The selenoenzyme phospholipid hydroperoxide glutathione peroxidase, Biochim. Biophys. Acta BBA - Gen. Subj. 839 (1985) 62–70, https://doi.org/10.1016/0304-4165(85)90182-5.

[17] M. Maiorino, K.-D. Aumann, R. Brigelius-Flohé, D. Doria, J. van den Heuvel, J. McCarthy, A. Roveri, F. Ursini, L. Flohé, Probing the presumed catalytic triad of selenium-containing peroxidases by mutational analysis of phospholipid hydroperoxide glutathione peroxidase (PHGPx), Biol. Chem. Hoppe Seyler 376 (1995) 651–660, https://doi.org/10.1515/bchm3.1995.376.11.651.

[18] M. Maiorino, F. Ursini, V. Bosello, S. Toppo, S.C.E. Tosatto, P. Mauri, K. Becker, A. Roveri, C. Bulato, L. Benazzi, A. De Palma, L. Flohé, The thioredoxin specificity of Drosophila GPx: a paradigm for a peroxiredoxin-like mechanism of many glutathione peroxidases, J. Mol. Biol. 365 (2007) 1033–1046, https://doi.org/10.1016/j.jmb.2006.10.033.

[19] S. Toppo, L. Flohé, F. Ursini, S. Vanin, M. Maiorino, Catalytic mechanisms and specificities of glutathione peroxidases: variations of a basic scheme, Biochim. Biophys. Acta BBA - Gen. Subj. 1790 (2009) 1486–1500, https://doi.org/10.1016/j.bbagen.2009.04.007.

[20] L. Flohé, J.R. Harris, Introduction. History of the peroxiredoxins and topical perspectives, Subcell. Biochem. 44 (2007) 1–25.

[21] S.G. Rhee, H.Z. Chae, K. Kim, Peroxiredoxins: a historical overview and speculative preview of novel mechanisms and emerging concepts in cell signaling, Free Radic. Biol. Med. 38 (2005) 1543–1552, https://doi.org/10.1016/j.freeradbiomed.2005.02.026.

[22] B. Söhling, T. Parther, K.P. Rücknagel, M. Wagner, J.R. Andreesen, A selenocysteine-containing peroxiredoxin from the strictly anaerobic organism eubacterium acidaminophilum, Biol. Chem. 382 (2001) 979–986, https://doi.org/10.1515/BC.2001.123.

[23] C.C. Winterbourn, The biological chemistry of hydrogen peroxide, Methods Enzymol, Elsevier, 2013, pp. 3–25, , https://doi.org/10.1016/B978-0-12-405881-1.00001-X.

[24] B. Cardey, M. Enescu, A computational study of thiolate and selenolate oxidation by hydrogen peroxide, ChemPhysChem 6 (2005) 1175–1180, https://doi.org/10.1002/cphc.200400568.

[25] A. Zeida, M. Trujillo, G. Ferrer-Sueta, A. Denicola, D.A. Estrin, R. Radi, Catalysis of peroxide reduction by fast reacting protein thiols: focus review, Chem. Rev. 119 (2019) 10829–10855, https://doi.org/10.1021/acs.chemrev.9b00371.

[26] B. Pedre, D. Young, D. Charlier, Á. Mourenza, L.A. Rosado, L. Marcos-Pascual, K. Wahni, E. Martens, A.G. de la Rubia, V.V. Belousov, L.M. Mateos, J. Messens, Structural snapshots of OxyR reveal the peroxidatic mechanism of H_2O_2 sensing, Proc. Natl. Acad. Sci. Unit. States Am. 115 (2018) E11623–E11632, https://doi.org/10.1073/pnas.1807954115.

[27] M. Trujillo, G. Ferrer-Sueta, L. Thomson, L. Flohé, R. Radi, L. Flohé, J.R. Harris (Eds.), Kinetics of Peroxiredoxins and Their Role in the Decomposition of Peroxynitrite, Peroxiredoxin Syst. Springer Netherlands, Dordrecht, 2007, pp. 83–113, , https://doi.org/10.1007/978-1-4020-6051-9_5.

[28] D.A. Meireles, R.M. Domingos, J.W. Gaiarsa, E.G. Ragnoni, R. Bannitz-Fernandes, J.F. da Silva Neto, R.F. de Souza, L.E.S. Netto, Functional and evolutionary characterization of Ohr proteins in eukaryotes reveals many active homologs among pathogenic fungi, Redox Biol 12 (2017) 600–609, https://doi.org/10.1016/j.redox.2017.03.026.

[29] L. Flohé, G. Loschen, W.A. Günzler, E. Eichele, Glutathione Peroxidase, V. The kinetic mechanism, Hoppe-Seyler's Z. Für Physiol. Chem. 353 (1972) 987–1000, https://doi.org/10.1515/bchm2.1972.353.1.987.

[30] L. Flohé, S. Toppo, G. Cozza, F. Ursini, A comparison of thiol peroxidase mechanisms, Antioxidants Redox Signal. 15 (2011) 763–780, https://doi.org/10.1089/ars.2010.3397.

[31] R. Brigelius-Flohé, L. Flohé, Basic principles and emerging concepts in the redox control of transcription factors, Antioxidants Redox Signal. 15 (2011) 2335–2381, https://doi.org/10.1089/ars.2010.3534.

[32] L. Flohé, The impact of thiol peroxidases on redox regulation, Free Radic. Res. 50 (2016) 126–142, https://doi.org/10.3109/10715762.2015.1046858.

[33] A. Delaunay, D. Pflieger, M.-B. Barrault, J. Vinh, M.B. Toledano, A thiol peroxidase is an H2O2 receptor and redox-transducer in gene activation, Cell 111 (2002) 471–481, https://doi.org/10.1016/S0092-8674(02)01048-6.

[34] B.A. Morgan, E.A. Veal, L. Flohé, J.R. Harris (Eds.), Functions of Typical 2-Cys Peroxiredoxins in Yeast, Peroxiredoxin Syst. Springer Netherlands, Dordrecht, 2007, pp. 253–265, , https://doi.org/10.1007/978-1-4020-6051-9_12.

[35] M.C. Sobotta, W. Liou, S. Stöcker, D. Talwar, M. Oehler, T. Ruppert, A.N.D. Scharf, T.P. Dick, Peroxiredoxin-2 and STAT3 form a redox relay for H2O2 signaling, Nat. Chem. Biol. 11 (2015) 64–70, https://doi.org/10.1038/nchembio.1695.

[36] K.D. Tew, Protein S-thonylation and glutathione S-transferase P, in: L. Flohé (Ed.), Glutathione, CRC Press, Boca Raton FL, 2019, pp. 201–313.

[37] S. Stöcker, M. Maurer, T. Ruppert, T.P. Dick, A role for 2-Cys peroxiredoxins in facilitating cytosolic protein thiol oxidation, Nat. Chem. Biol. 14 (2018) 148–155, https://doi.org/10.1038/nchembio.2536.

[38] M.F. Christman, R.W. Morgan, F.S. Jacobson, B.N. Ames, Positive control of a regulon for defenses against oxidative stress and some heat-shock proteins in Salmonella typhimurium, Cell 41 (1985) 753–762, https://doi.org/10.1016/S0092-8674(85)80056-8.

[39] T. Hildebrandt, J. Knuesting, C. Berndt, B. Morgan, R. Scheibe, Cytosolic thiol switches regulating basic cellular functions: GAPDH as an information hub? Biol. Chem. 396 (2015) 523–537, https://doi.org/10.1515/hsz-2014-0295.

[40] G. Ferrer-Sueta, B. Manta, H. Botti, R. Radi, M. Trujillo, A. Denicola, Factors affecting protein thiol reactivity and specificity in peroxide reduction, Chem. Res. Toxicol. 24 (2011) 434–450, https://doi.org/10.1021/tx100413v.

[41] C.C. Winterbourn, M.B. Hampton, Thiol chemistry and specificity in redox signaling, Free Radic. Biol. Med. 45 (2008) 549–561, https://doi.org/10.1016/j.freeradbiomed.2008.05.004.

[42] D. Peralta, A.K. Bronowska, B. Morgan, É. Dóka, K. Van Laer, P. Nagy, F. Gräter, T.P. Dick, A proton relay enhances H_2O_2 sensitivity of GAPDH to facilitate metabolic adaptation, Nat. Chem. Biol. 11 (2015) 156–163, https://doi.org/10.1038/nchembio.1720.

[43] L. Orian, P. Mauri, A. Roveri, S. Toppo, L. Benazzi, V. Bosello-Travain, A. De Palma, M. Maiorino, G. Miotto, M. Zaccarin, A. Polimeno, L. Flohé, F. Ursini, Selenocysteine oxidation in glutathione peroxidase catalysis: an MS-supported quantum mechanics study, Free Radic. Biol. Med. 87 (2015) 1–14, https://doi.org/10.1016/j.freeradbiomed.2015.06.011.

[44] L.A.H. van Bergen, M. Alonso, A. Palló, L. Nilsson, F. De Proft, J. Messens, Revisiting sulfur H-bonds in proteins: the example of peroxiredoxin AhpE, Sci. Rep. 6 (2016) 30369, https://doi.org/10.1038/srep30369.

[45] J.L. Jenkins, J.J. Tanner, High-resolution structure of human D -glyceraldehyde-3-phosphate dehydrogenase, Acta Crystallogr. D Biol. Crystallogr. 62 (2006) 290–301, https://doi.org/10.1107/S0907444905042289.

[46] I. Jo, I.-Y. Chung, H.-W. Bae, J.-S. Kim, S. Song, Y.-H. Cho, N.-C. Ha, Structural details of the OxyR peroxide-sensing mechanism, Proc. Natl. Acad. Sci. Unit. States Am. 112 (2015) 6443–6448, https://doi.org/10.1073/pnas.1424495112.

[47] M.J. Frisch, G.W. Trucks, H.B. Schlegel, G.E. Scuseria, M.A. Robb, J.R. Cheeseman, G. Scalmani, V. Barone, G.A. Petersson, H. Nakatsuji, X. Li, M. Caricato, A.V. Marenich, J. Bloino, B.G. Janesko, R. Gomperts, B. Mennucci, H.P. Hratchian, J.V. Ortiz, A.F. Izmaylov, J.L. Sonnenberg, Williams, F. Ding, F. Lipparini, F. Egidi, J. Goings, B. Peng, A. Petrone, T. Henderson, D. Ranasinghe, V.G. Zakrzewski, J. Gao, N. Rega, G. Zheng, W. Liang, M. Hada, M. Ehara, K. Toyota, R. Fukuda, J. Hasegawa, M. Ishida, T. Nakajima, Y. Honda, O. Kitao, H. Nakai, T. Vreven, K. Throssell, J.A. Montgomery Jr., J.E. Peralta, F. Ogliaro, M.J. Bearpark, J.J. Heyd, E.N. Brothers, K.N. Kudin, V.N. Staroverov, T.A. Keith, R. Kobayashi, J. Normand, K. Raghavachari, A.P. Rendell, J.C. Burant, S.S. Iyengar, J. Tomasi, M. Cossi, J.M. Millam, M. Klene, C. Adamo, R. Cammi, J.W. Ochterski, R.L. Martin, K. Morokuma, O. Farkas, J.B. Foresman, D.J. Fox, Gaussian 16, Rev. C.01, Wallingford, CT, 2016.

[48] A.D. Becke, Density-functional thermochemistry. III. The role of exact exchange, J. Chem. Phys. 98 (1993) 5648–5652, https://doi.org/10.1063/1.464913.

[49] C. Lee, W. Yang, R.G. Parr, Development of the Colle-Salvetti correlation-energy formula into a functional of the electron density, Phys. Rev. B 37 (1988) 785–789, https://doi.org/10.1103/PhysRevB.37.785.

[50] P.J. Stephens, F.J. Devlin, C.F. Chabalowski, M.J. Frisch, Ab initio calculation of vibrational absorption and circular dichroism spectra using density functional force fields, J. Phys. Chem. 98 (1994) 11623–11627, https://doi.org/10.1021/j100096a001.

[51] S.H. Vosko, L. Wilk, M. Nusair, Accurate spin-dependent electron liquid correlation energies for local spin density calculations: a critical analysis, Can. J. Phys. 58 (1980) 1200–1211, https://doi.org/10.1139/p80-159.

[52] S. Grimme, J. Antony, S. Ehrlich, H. Krieg, A consistent and accurate ab initio parametrization of density functional dispersion correction (DFT-D) for the 94 elements H-Pu, J. Chem. Phys. 132 (2010) 154104, , https://doi.org/10.1063/1.3382344.

[53] S. Grimme, S. Ehrlich, L. Goerigk, Effect of the damping function in dispersion corrected density functional theory, J. Comput. Chem. 32 (2011) 1456–1465, https://doi.org/10.1002/jcc.21759.

[54] R. Krishnan, J.S. Binkley, R. Seeger, J.A. Pople, Self-consistent molecular orbital methods. XX. A basis set for correlated wave functions, J. Chem. Phys. 72 (1980) 650–654, https://doi.org/10.1063/1.438955.

[55] A.D. McLean, G.S. Chandler, Contracted Gaussian basis sets for molecular calculations. I. Second row atoms, $Z=11$–18, J. Chem. Phys. 72 (1980) 5639–5648, https://doi.org/10.1063/1.438980.

[56] N.J. DeYonker, K.A. Peterson, A.K. Wilson, Systematically convergent correlation consistent basis sets for molecular Core − Valence correlation effects: the third-row atoms gallium through krypton, J. Phys. Chem. 111 (2007) 11383–11393, https://doi.org/10.1021/jp0747757.

[57] F. Neese, The ORCA program system, WIREs Comput. Mol. Sci. 2 (2012) 73–78, https://doi.org/10.1002/wcms.81.

[58] F. Neese, Software update: the ORCA program system, version 4.0, WIREs Comput, Mol. Sci. 8 (2018), https://doi.org/10.1002/wcms.1327.

[59] A.V. Marenich, C.J. Cramer, D.G. Truhlar, Universal solvation model based on solute electron density and on a continuum model of the solvent defined by the bulk dielectric constant and atomic surface tensions, J. Phys. Chem. B 113 (2009) 6378–6396, https://doi.org/10.1021/jp810292n.

[60] M. Bortoli, M. Torsello, F.M. Bickelhaupt, L. Orian, Role of the chalcogen (S, Se, Te) in the oxidation mechanism of the glutathione peroxidase active site, ChemPhysChem 18 (2017) 2990–2998, https://doi.org/10.1002/cphc.201700743.

[61] L. Li, C. Li, Z. Zhang, E. Alexov, On the dielectric "constant" of proteins: smooth dielectric function for macromolecular modeling and its implementation in DelPhi, J. Chem. Theor. Comput. 9 (2013) 2126–2136, https://doi.org/10.1021/ct400065j.

[62] A. Zeida, C.M. Guardia, P. Lichtig, L.L. Perissinotti, L.A. Defelipe, A. Turjanski, R. Radi, M. Trujillo, D.A. Estrin, Thiol redox biochemistry: insights from computer simulations, Biophys. Rev. 6 (2014) 27–46, https://doi.org/10.1007/s12551-013-0127-x.

[63] B. Pedre, L.A.H. van Bergen, A. Palló, L.A. Rosado, V.T. Dufe, I.V. Molle, K. Wahni, H. Erdogan, M. Alonso, F.D. Proft, J. Messens, The active site architecture in peroxiredoxins: a case study on Mycobacterium tuberculosis AhpE, Chem. Commun. 52 (2016) 10293–10296, https://doi.org/10.1039/C6CC02645A.

[64] L. Flohé, H. Budde, K. Bruns, H. Castro, J. Clos, B. Hofmann, S. Kansal-Kalavar, D. Krumme, U. Menge, K. Plank-Schumacher, H. Sztajer, J. Wissing, C. Wylegalla, H.-J. Hecht, Tryparedoxin peroxidase of Leishmania donovani: molecular cloning, heterologous expression, specificity, and catalytic mechanism, Arch. Biochem. Biophys. 397 (2002) 324–335, https://doi.org/10.1006/abbi.2001.2688.

[65] C. Fonseca Guerra, F.M. Bickelhaupt, J.G. Snijders, E.J. Baerends, The nature of the hydrogen bond in DNA base pairs: the role of charge transfer and resonance assistance, Chem. Eur J. 5 (1999) 3581–3594, https://doi.org/10.1002/(SICI)1521-3765(19991203)5:12<3581:AID-CHEM3581>3.0.CO;2-Y.

[66] L.P. Wolters, F.M. Bickelhaupt, Halogen bonding versus hydrogen bonding: a molecular orbital perspective, ChemistryOpen 1 (2012) 96–105, https://doi.org/10.1002/open.201100015.

[67] A. Hall, D. Parsonage, L.B. Poole, P.A. Karplus, Structural evidence that peroxiredoxin catalytic power is based on transition-state stabilization, J. Mol. Biol. 402 (2010) 194–209, https://doi.org/10.1016/j.jmb.2010.07.022.

[68] A. Zeida, A.M. Reyes, M.C.G. Lebrero, R. Radi, M. Trujillo, D.A. Estrin, The extraordinary catalytic ability of peroxiredoxins: a combined experimental and QM/MM study on the fast thiol oxidation step, J. Chem. Soc., Chem. Commun. 50 (2014) 10070–10073, https://doi.org/10.1039/C4CC02899F.

[69] E. Cuevasanta, A.M. Reyes, A. Zeida, M. Mastrogiovanni, M.I. De Armas, R. Radi, B. Alvarez, M. Trujillo, Kinetics of formation and reactivity of the persulfide in the one-cysteine peroxiredoxin from *Mycobacterium tuberculosis*, J. Biol. Chem. 294 (2019) 13593–13605, https://doi.org/10.1074/jbc.RA119.008883.

[70] E. Derat, S. Shaik, C. Rovira, P. Vidossich, M. Alfonso-Prieto, The effect of a water molecule on the mechanism of formation of compound 0 in horseradish peroxidase, J. Am. Chem. Soc. 129 (2007) 6346–6347, https://doi.org/10.1021/ja0676861.

[71] P. Vidossich, G. Fiorin, M. Alfonso-Prieto, E. Derat, S. Shaik, C. Rovira, On the role of water in peroxidase catalysis: a theoretical investigation of HRP compound I formation, J. Phys. Chem. B 114 (2010) 5161–5169, https://doi.org/10.1021/jp911170b.